Check for updates

CHEMMEDCHEM

CHEMISTRY ENABLING DRUG DISCOVERY

Accepted Article

Title: Structure-Activity Relationship Studies on (R)-PFI-2 Analogs as Inhibitors of Histone Lysine Methyltransferase SETD7

Authors: Danny C Lenstra, Eddy Damen, Ruben G. G. Leenders, Richard H. Blaauw, Floris P. J. T. Rutjes, Anita Wegert, and Jasmin Mecinovic

This manuscript has been accepted after peer review and appears as an Accepted Article online prior to editing, proofing, and formal publication of the final Version of Record (VoR). This work is currently citable by using the Digital Object Identifier (DOI) given below. The VoR will be published online in Early View as soon as possible and may be different to this Accepted Article as a result of editing. Readers should obtain the VoR from the journal website shown below when it is published to ensure accuracy of information. The authors are responsible for the content of this Accepted Article.

To be cited as: *ChemMedChem* 10.1002/cmdc.201800242

Link to VoR: http://dx.doi.org/10.1002/cmdc.201800242

A Journal of

ChemPubSoc Europe

WILEY-VCH

www.chemmedchem.org

10.1002/cmdc.201800242

WILEY-VCH

FULL PAPER

Structure-Activity Relationship Studies on (*R*)-PFI-2 Analogs as Inhibitors of Histone Lysine Methyltransferase SETD7

Danny C. Lenstra,[a] Eddy Damen,[b] Ruben G. G. Leenders,[b] Richard H. Blaauw,[c] Floris P. J. T. Rutjes,[a] Anita Wegert,[b] and Jasmin Mecinović*[a]

[a] D. C. Lenstra, Prof. Dr. F. P. J. T. Rutjes, Dr. J. Mecinović
Institute for Molecules and Materials, Radboud University
Heyendaalseweg 135, 6525 AJ Nijmegen, The Netherlands
E-mail: j.mecinovic@science.ru.nl
[b] Dr. E. Damen, Dr. R. G. G. Leenders, Dr. A. Wegert
Mercachem BV
Kerkenbos 1013, 6546 BB Nijmegen, The Netherlands
[c] Dr. R. H. Blaauw
Chiralix
Toernooiveld 100, 6525 EC Nijmegen, The Netherlands

Supporting information for this article is given via a link at the end of the document.

Abstract: SETD7 is a histone H3K4 lysine methyltransferase involved in human gene regulation. Aberrant expression of SETD7 has been associated with various diseases, including cancer, therefore SETD7 is considered as a target for the development of new epigenetic drugs. To date, few selective small molecule inhibitors have been reported that target SETD7, the most potent being (*R*)-PFI-2. Here we report structure-activity relationship studies on (*R*)-PFI-2 and its analogs. A library of 29 structural analogs of (*R*)-PFI-2 was synthesized and evaluated for inhibition of recombinantly expressed human SETD7. The key interactions were found to be a salt-bridge and a hydrogen bond formed between (*R*)-PFI-2's NH_2^+ and SETD7's Asp256 and His252, respectively.

Introduction

Covalent posttranslational modifications on the unstructured N-terminal histone tails play an important role in regulating the activity of human genes.[1] These modifications are introduced by 'writers' and, among others, include methylation, acetylation, phosphorylation, citrullination, and ubiquitination.[2] Methylation is one of the most abundant and well-studied modifications on histones.[3] The transfer of a methyl group from cosubstrate S-adenosylmethionine (SAM) to lysine residues is catalyzed by histone lysine methyltransferases (KMTs).[4] KMTs can catalyze the addition of up to three methyl groups to the ε-amino group of lysine residues, affording methyllysine (Kme), dimethyllysine (Kme2) and trimethyllysine (Kme3).[5] With the exception of DOT1L, an H3K79 methyltransferase, all KMTs contain a highly conserved SET (Su(var)3-9, enchanter-of-zeste, thritorax) domain, which is responsible for their catalytic activity.[6]

SET domain containing lysine methyltransferase 7 (SETD7, also known as SET7/9) was originally identified as a monomethylase of lysine 4 on histone 3 (H3K4).[7] Unlike many other methyltransferases, SETD7 only monomethylates H3K4, but does not catalyze di- or trimethylation of lysine. This methylation mark (H3K4me) has a functional effect on the chromatin state resulting in activation of transcription. SETD7 has also been found to catalyze methylation of a range of non-histone proteins, including estrogen receptor α (ERα)[8], DNA

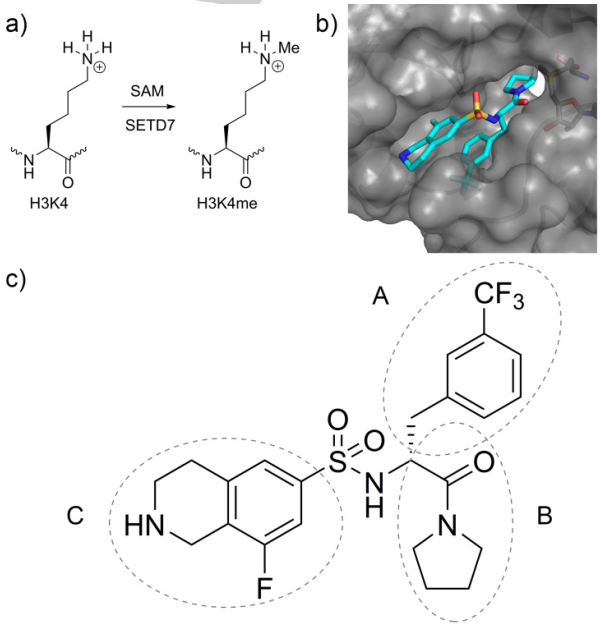

Figure 1. a) SETD7-catalyzed methylation of H3K4; b) Crystal structure of SETD7 (grey) in complex with (*R*)-PFI-2 (cyan) (PDB ID: 4JLG); c) Structure of (*R*)-PFI-2, with sites A, B, and C for SAR exploration.

methyltransferases 1 (DNMT1)[9], TAF10[10], FoxO3[11], transcription factors YY1 and Pdx1[12], androgen receptor[13], ARTD1[14], beta-catenin[15], and tumor suppressor p53[16]. Recent biomedical studies revealed that SETD7 is involved in multiple signaling pathways, and its aberrant activity has been linked to various types of cancer[17] and vascular dysfunction in patients with type 2 diabetes[18]. The development of SETD7 small molecule inhibitors as chemical probes for studying their biological activity in cells is therefore highly desired and may lead to the development of therapeutic agents for the treatment of human diseases.[19]

To date, only a few selective SETD7 inhibitors have been identified. Clinically approved antihistaminic cyproheptadine was found to inhibit SETD7-mediated methylation of H3K4 (IC_{50} of 3.4

Accepted Manuscript

This article is protected by copyright. All rights reserved.

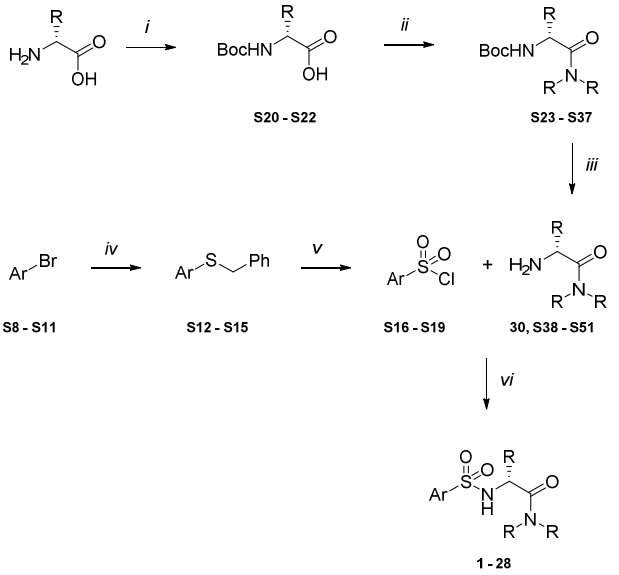

Scheme 1. Syntheses of (*R*)-PFI-2 and its analogs **1**-**28**. Reagents and conditions: *i*) Boc_2O, and NaOH in H_2O/dioxane (1:1 *v*/*v*), rt, 20 h; *ii*) EDCI, HOBt, DIPEA, and R_2NH in DCM, rt, 20 h; *iii*) TFA/DCM (1:1 *v*/*v*), rt, 2-4 h; *iv*) $Pd_2(dba)_3$, Xantphos, DIPEA, and benzylmercaptan in dioxane, 100 °C, 6 h; *v*) Benzyltrimethylammonium chloride, trichloroisocyanuric acid, and Na_2CO_3 in H_2O/MeCN, 0 °C to rt, 1 h; *vi*) Et_3N in DCM, rt, 4 h. Where applicable, Boc-protected compounds were deprotected using TFA/DCM (1:1 *v*/*v*).

μM). The substrate in this study was ERα, and *in vivo* inhibition led to blocking of estrogen-dependent breast cancer cell growth in MCF7 cells.[20] A structure-activity relationship study was performed, however, none of the analogs proved to be more potent than cyproheptadine.[21] Several SAM derivatives have also been reported to inhibit SETD7 methyltransferase activity; for instance, DAAM-3 (IC_{50} 10 μM)[22] and DC-S239 (IC_{50} 4.59 μM).[23] Unfortunately, SAM-competitive inhibitors usually have poor selectivity amongst other methyltransferases due to the highly conserved SAM binding domain in the methyltransferase family. The most potent known SETD7 inhibitor (IC_{50} = 2.0 ± 0.2 nM) is (*R*)-PFI-2 (Figure 1b-c), while its enantiomer (*S*)-PFI-2 proved to be a very weak SETD7 inhibitor, highlighting that the stereochemistry of the amino acid side chain defines its potency.[24] (*R*)-PFI-2 is a histone competitive inhibitor, and exhibits an inhibition potency *in vitro* and in cellular assays.[24] Comparative studies demonstrated that (*R*)-PFI-2 is selective for SETD7 over 18 other human methyltransferases. Although the structure of (*R*)-PFI-2 in complex with SETD7 has been solved (Figure 1b), no further analogs have been reported. To investigate which structural elements of (*R*)-PFI-2 are essential for effective inhibition of SETD7, we carried out a structure-activity relationship (SAR) study. We modified three distinctive moieties that have a potential to crucially contribute to the potency of (*R*)-PFI-2: *i*) The amino acid side chain (Figure 1c, part A); *ii*) the pyrrolidine amide (Figure 1c, part B); and *iii*) the tetrahydroisoquinoline moiety (Figure 1c, part C).

Results and Discussion

We initiated our investigations with the synthesis of (*R*)-PFI-2 (**1**) and its 29 structural analogs (Scheme 1). In general, the synthesis was adapted from literature,[24] and starts from an unnatural D-amino acid; typically Boc-protected D-phenylalanine derivatives were coupled to the requisite amines using EDCI, HOBt, and DIPEA. Then the Boc group was removed with TFA in DCM, followed by a basic work-up to afford the free amine. The sulfonyl part of the inhibitor was synthesized from various aryl bromides (Scheme 1). These aryl bromides were first reacted with benzyl mercaptan in the presence of $Pd_2(dba)_3$ and Xantphos to afford aryl benzyl sulfides, followed by oxidation with trichloroisocyanuric acid to yield the corresponding sulfonyl chlorides. The sulfonyl chlorides were then coupled to the free amines in the presence of triethylamine in DCM to afford the desired structural analogs of (*R*)-PFI-2.

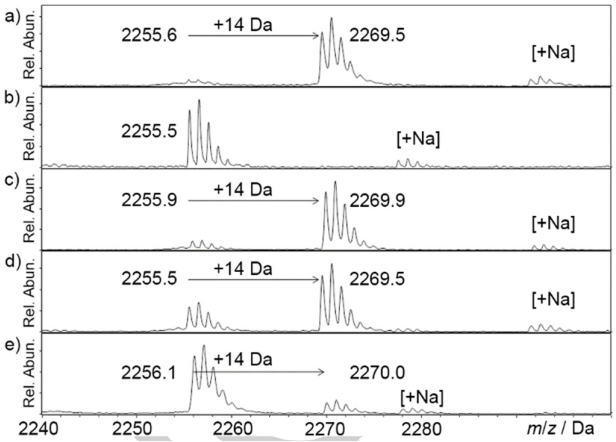

Figure 2. a) Representative MALDI-TOF MS data for 200 nM SETD7, 21-mer H3K4 peptide (10 μM), SAM (16 μM) in 50 mM glycine pH 8.8 containing 2.5% glycerol and 5% DMSO (*v*/*v*) after 1 h at 37 °C; b) 10 μM of (*R*)-PFI-2 (compound **1**); c) 10 μM compound **9**; d) 10 μM compound **14**; e) 10 μM compound **27**. Y-axis represents relative abundance (Rel. abun.).

Initially, all synthesized compounds were tested for their inhibitory activity using an established matrix-assisted laser desorption-ionization time-of-flight mass spectrometry (MALDI-TOF MS) assay, monitoring the monomethylation of a synthetic 21-mer histone 3 peptide mimic containing a lysine at position 4.[25] In a typical assay, 200 nM of SETD7, 10 μM of H3K4 histone peptide, 16 μM of SAM and 10 or 100 μM of compounds **1**-**30** were incubated for 1 hour at 37 °C. For compounds showing >50% inhibition at 100 μM, IC_{50}s were determined. In cases where <50% inhibition at 100 μM was observed, IC_{50}s were not determined and this data is presented as IC_{50} >100 μM. Enzymatic activity of these compounds at 100 μM concentration can be found in Figure S1 in Supporting Information. Representative MALDI data of selected compounds at 10 μM are shown in Figure 2. In a control experiment without inhibitor (5% (*v*/*v*) of DMSO) nearly quantitative methylation was observed in the presence of human SETD7 (*m*/*z* = 2269.5) (Figure 2a). Under standard conditions, but in the presence of 10 μM of (*R*)-PFI-2 (compound **1**), no methylation was observed in the MALDI spectrum (Figure 2b).

We further examined the potency of (*R*)-PFI-2 against recombinantly expressed human SETD7. Under our assay conditions, an IC_{50} value of 138 nM was obtained for (*R*)-PFI-2 (Figure 3, compound **1**), indicating very effective inhibition of SETD7 methyltransferase activity. Previously reported IC_{50} values for (*R*)-PFI-2 were 2.0 and 55 nM, respectively;[24, 25b] the observed difference with our measured IC_{50} value is due to differences in employed assay and assay conditions. Representative inhibition curves can be found in Figure S2. Two isomers of **1**, with *ortho*- (compound **2**) and *para*-CF_3 (compound

This article is protected by copyright. All rights reserved.

Accepted Manuscript

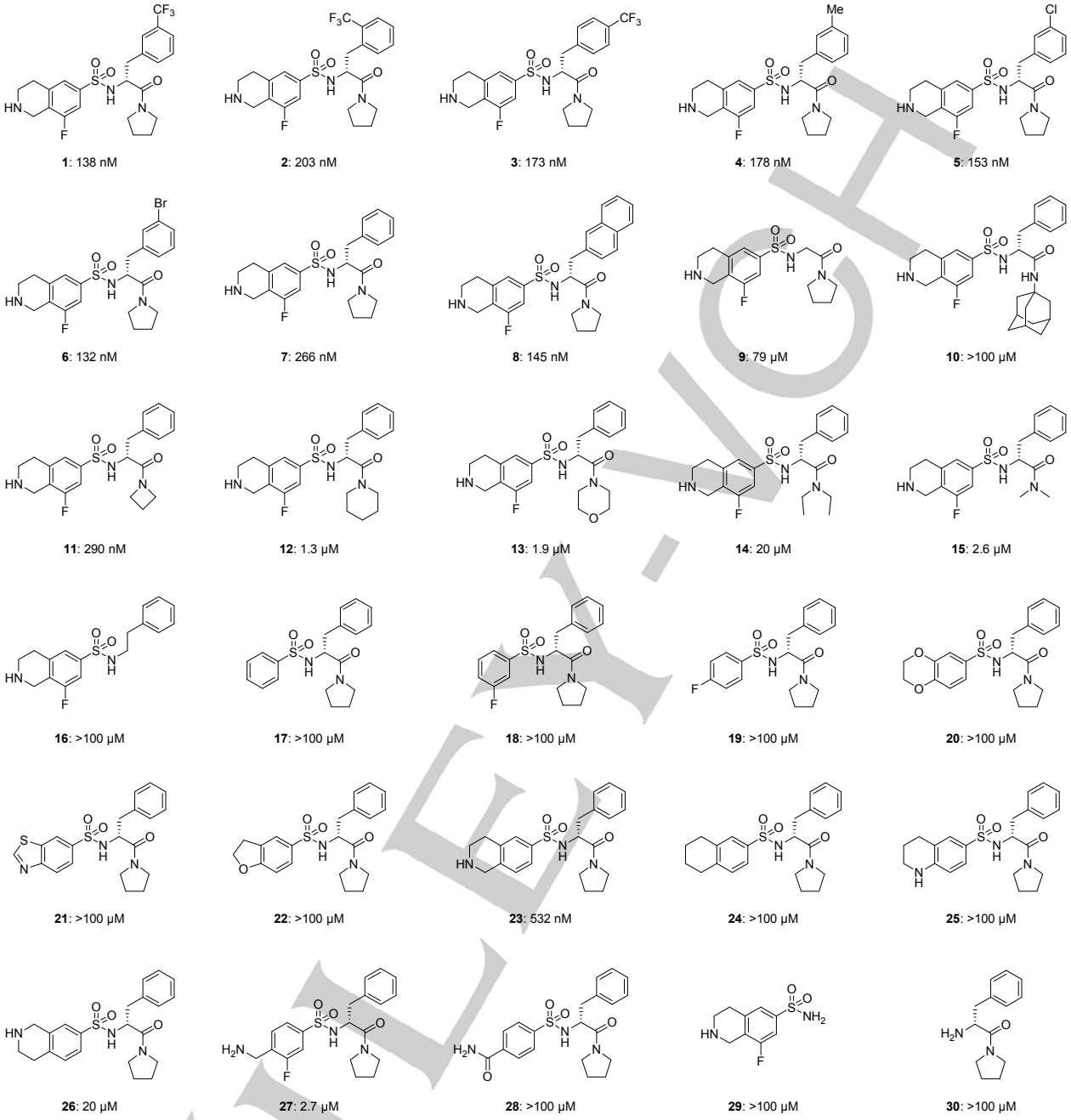

Figure 3. A library of (*R*)-PFI-2 (compound **1**) and its analogs **2**-**30**, showing the maximum half inhibitory concentrations (IC_{50}s).

3) substituents also displayed excellent inhibitory activity with an IC_{50} of 203 and 173 nM, respectively. The potencies of analogs **4**-**6** bearing a methyl-, chloro-, or bromo functionality at the *meta*-position were evaluated next. All compounds were found to be excellent inhibitors of SETD7 with IC_{50}s ranging from 132 nM to 178 nM. Also compound **7**, which does not contain any substituent on the phenyl ring, was found to be a good SETD7 inhibitor with an IC_{50} of 266 nM. Adding an extra fused ring, as in the naphthalene-containing compound **8**, gave an IC_{50} of 145 nM, indicating that there is sufficient space available for additional functionalization. Notably, removing the entire side chain (as in glycine-based compound **9**) led to rather poor inhibition with an IC_{50} of 79 μM, implying that the aromatic ring is crucial for potency.

Next, the effect of modifications in the pyrrolidine amide side chain was investigated (Figure 1c, part B). The analysis of the crystal structure of (*R*)-PFI-2 as cocrystal with SETD7 and SAM (PDB ID: 4JLG) illustrates that the pyrrolidine part of the inhibitor is positioned inside the lysine channel pointing towards SAM (Figure 1b). Based on this structural information, it is clear that space in this pocket is limited and that a significant increase in the size of the pyrrolidine moiety would presumably not be tolerated. Indeed, 1-adamantyl substituted compound **10** did not show any inhibitory activity against SETD7. No significant difference in IC_{50}

This article is protected by copyright. All rights reserved.

Accepted Manuscript

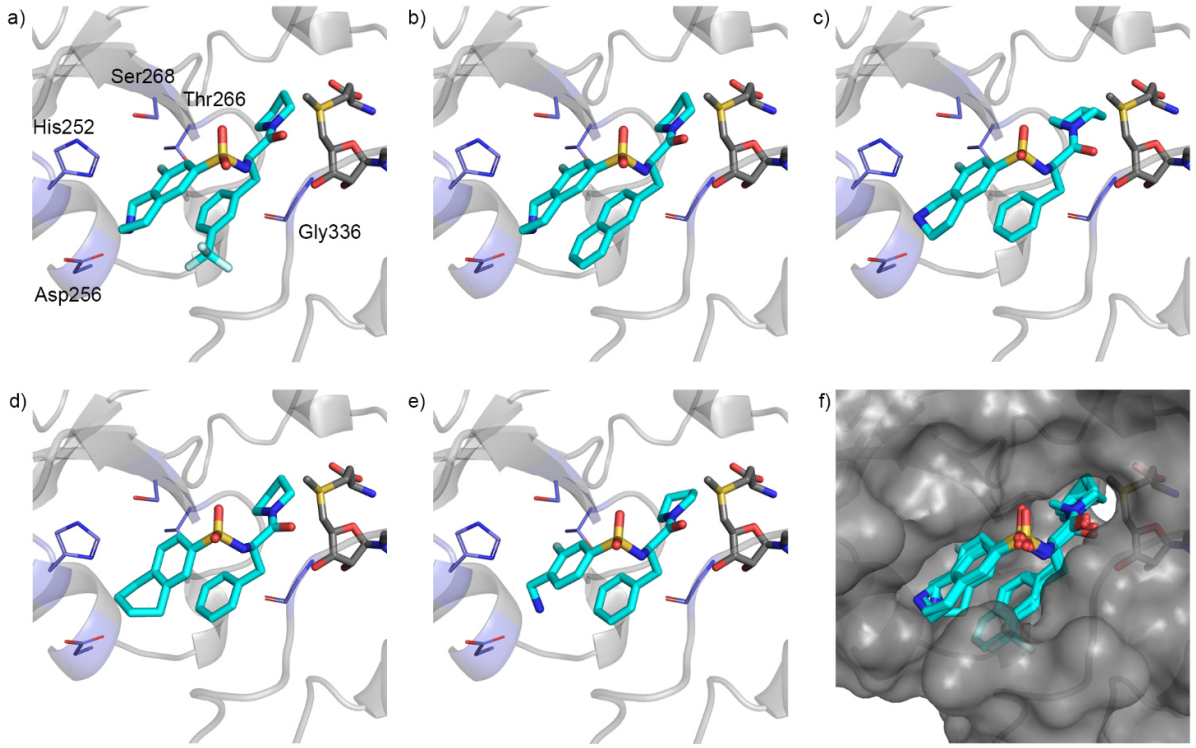

Figure 4. Docking studies on various (*R*)-PFI-2 analogs (cyan) with SETD7 (cartoon, grey) with SAM (grey). SETD7 residues that form key interactions are shown in purple: a) Redocked structure of (*R*)-PFI-2 (compound **1**), RMSD = 0.638; b) docking of compound **8**, containing a naphthalene side chain; c) docking of compound **12**, containing a piperidine amide functionality; d) docking of carbon analog **24**; e) docking of benzylamine-type compound **27**; f) superimposition of structures shown in Figures 4a-e, with SETD7 surface visualization (grey).

was observed when the 5-membered ring of the pyrrolidine amide (compound **7**, 266 nM) was replaced by a 4-membered ring: an IC_{50} of 290 nM was obtained for azetidine derived analog **11**. By slightly increasing the ring size to piperidine or morpholine amide, as in analogs **12** and **13**, IC_{50}s of 1.3 and 1.9 µM were observed, respectively. This result shows that a slight increase in ring size from a 5- to 6-membered already leads to an ~5-fold drop in potency (compound **7** vs. **12**). Replacement of the 5-membered ring with acyclic diethylamine derivative **14**, resulted in a higher degree of rotational freedom, which could lead to a steric clash with SETD7's pocket; this proposition is in line with a surprisingly higher IC_{50} value of 20 µM. An almost 10-fold lower IC_{50} of 2.6 µM was obtained by decreasing the size and rotational freedom in dimethylamine derivative **15**. Removal of the entire pyrrolidine amide side chain (as in compound **16**), resulted in the formation of an achiral compound. This significant structural change caused that **16** is no longer an inhibitor of SETD7 within limits of detection.

Finally, the importance of the tetrahydroisoquinoline rings was investigated (Figure 1c, part C). The simplest analogs **17**-**19**, consisting of a phenyl ring, either unsubstituted or with fluorine on the *meta*- or *para*-position, did not significantly inhibit SETD7 methyltransferase activity, indicating the essential role of the tetrahydroisoquinoline scaffold of (*R*)-PFI-2 in inhibition of SETD7. IC_{50} values of >100 µM were observed for several heteroatom-substituted analogs **20**-**22**, containing for instance a planar or nonplanar heterocyclic system. To investigate the importance of the fluorine substituent, we synthesized analog **23**, which has an IC_{50} value of 532 nM; this is approximately a two-fold increase with respect to fluorine-containing compound **7** (IC_{50} = 266 nM). Approximately 10% inhibition of methyltransferase activity was observed in the presence of 100 µM of compound **24**, an analog of **7** that has the positively charged quaternary ammonium group (under physiological conditions) replaced by a neutral methylene group of equal size (Figure S1). This result demonstrates that the positively charged NH_2^+ of (*R*)-PFI-2's is involved in two interactions with SETD7, namely as a salt-bridge with Asp252 and a hydrogen bond with His252. Notably, when this nitrogen was translocated one position, as in tetrahydroquinoline **25**, again no inhibition was observed, whereas for compound **26**, only a poor inhibition with an IC_{50} value of 20 µM was seen. Based on our examination of compounds **23**-**26**, it is clearly evident that the most important contributor to the excellent potency of (*R*)-PFI-2 is the nitrogen-containing tetrahydroisoquinoline functionality. Having a benzylamine moiety instead of the cyclic structure, as in compound **27**, a moderately active compound is obtained (IC_{50} = 2.7 µM). With compound **28**, a formation of a salt-bridge is no longer possible after changing the free amine to an amide functionality, and consequently no inhibition was observed. The two individual fragments of which the (*R*)-PFI-2 scaffold consists also showed no inhibitory activity (Figure 3, compounds **29** and **30**).

Docking studies were then carried out to obtain more detailed information about the potential binding modes of various (*R*)-PFI-2 analogs (Figures 4a-f). Initially, to confirm the correct docking mode, (*R*)-PFI-2 was successfully redocked into the structure of SETD7 (RMSD = 0.638 Å, Figure 4a). The ligand interaction diagram for SETD7–(*R*)-PFI-2 is shown in Figure S3. Compound **8** was docked into SETD7 and the binding mode of **8** was found to be similar to that of (*R*)-PFI-2 (Figure 4b). In the docked structure of **12,** the piperidine group occupies the narrow

Accepted Manuscript
This article is protected by copyright. All rights reserved.

lysine-binding channel; although it is somewhat larger than (*R*)-PFI-2's pyrrolidine group, **12** does not noticeably clash with the protein (Figure 4c). Finally, two structures with the tetrahydroisoquinoline core were docked. Despite being a very poor inhibitor of SETD7 (10% inhibition at 100 µM, Figure S1), docking of the carbon analog **24** was successful and the apparent binding mode seems similar to that of (*R*)-PFI-2, in spite of the absence of interactions with Asp256 and His252 (Figure 4d). In contrast, the benzylamine-derived compound **27** does have a potential to form a salt-bridge with Asp256 and a hydrogen bond with His252 under physiological conditions, and docking of this molecule into SETD7 confirmed the existence of the energetically favorable salt-bridge and hydrogen bond (Figure 4e).

Conclusions

A library of 29 (*R*)-PFI-2 analogs was synthesized and evaluated as SETD7 inhibitors with the aim to determine which structural features contribute to the excellent potency of (*R*)-PFI-2. Our results demonstrate that small perturbations in the pyrrolidine amide side chain, *i.e.* piperidine amide **12** or dimethylamide **15** were tolerated relatively well, whereas substituents with more rotational freedom (e.g. diethylamide **14**) or with increased size (e.g. adamantane **10**) were not tolerated. Substitutions on the aromatic side chain led to highly potent (*R*)-PFI-2 analogs. The key interactions between SETD7 and (*R*)-PFI-2 were identified to be a salt-bridge and a hydrogen bond that are formed between SETD7's Asp256/His252 and the tetrahydroisoquinoline's NH_2^+ of (*R*)-PFI-2. Removal or repositioning of this ammonium group resulted in analogs that were inactive (compounds **24** and **25**) or only poorly active (compound **26**), whereas a replacement of the tetrahydroisoquinoline moiety by benzylamine (as in compound **27**) resulted in an ~10 times less potent inhibitor. It is envisioned that this study will importantly contribute to the growing field of epigenetic drug discovery.

Experimental Section

Inhibition studies.

For determination of maximum half inhibitory concentrations (IC_{50}s), a MALDI-TOF MS based assay monitoring methylation of a 21-mer histone 3 peptide mimic containing a lysine at position 4 was used. Briefly, SETD7 (200 nM final concentration) was preincubated with compound (100% DMSO stock solution at appropriate concentration) for 5 minutes at 37 °C in 18 µL of 50 mM glycine pH 8.8 containing 2.5% glycerol as assay buffer. Then, 2 µL of SAM (16 µM final concentration) and 21-mer H3K4 peptide (10 µM final concentration) premixture was added to initiate the enzymatic reaction, thereby obtaining a final reaction volume of 20 µL containing 5% DMSO (*v/v*). The reaction was left to incubate for an additional 1 hour at 37 °C after which it was quenched by the addition of 20 µL of methanol. For MALDI-TOF MS analysis, a 2 µL aliquot from the quenched reaction mixture was mixed with 8 µL of saturated HCCA matrix (α-cyano-4-hydroxycinnamic acid, Sigma-Aldrich). From this mixture 1 µL was deposited on the MALDI plate for crystallization. Methyltransferase activity was calculated by taking the peak area of monomethylation state (including all isotopes and adducts), and is expressed relative to the reaction in which no compound was present (control experiment in which just 5% DMSO was present). The calculated activities were plotted against the corresponding compound concentrations and fitted to the Hill-equation using Origin Pro. Each experiment was performed in triplicate.

Docking studies.

The crystal structure of SETD7 in complex with (*R*)-PFI-2 and S-adenosylmethionine (SAM)[24] was downloaded from the Protein Data Bank (PDB ID: 4JLG). The protein-ligand complex (chain A) was prepared for docking using the QuickPrep wizard in Molecular Operating Environment (MOE).[26] All compounds to be docked were prepared using the default settings of the Wash wizard as implemented in MOE. Molecular docking was performed using Molegro Virtual Docker v6.0.[27] The active binding site region was defined as a spherical region, which encompasses all protein within 10.0 Å of bound (*R*)-PFI-2. Both the MolDock Score [GRID] and PLANTS Score [GRID] with a grid resolution of 0.2 Å were evaluated to score and rank the 5 best docking poses for each compound. MolDock SE was selected as search algorithm using its default settings. All figures we prepared with PyMOL visualization software.[28]

Characterization of final compounds.

Compound **1** (25 mg, 75% isolated yield, off-white solid): ^{1}H NMR (400 MHz, $CDCl_3$) δ 7.51 – 7.46 (m, 1H), 7.40 – 7.35 (m, 2H), 7.33 – 7.31 (m, 2H), 7.19 (d, *J* = 8.7, 1H), 4.19 (t, *J* = 7.5, 1H), 4.03 (bs, 2H), 3.22 – 3.06 (m, 5H), 2.99 (d, *J* = 7.5, 2H), 2.86 – 2.75 (m, 2H), 2.59 – 2.47 (m, 1H), 1.76 – 1.52 (m, 4H), 1.25 (bs, 1H); ^{13}C NMR (101 MHz, $CDCl_3$) δ 168.3, 160.0, 157.5, 139.0, 138.9, 138.8, 138.7, 136.7, 133.0, 133.0, 131.3, 131.0, 130.7, 130.3, 129.0, 128.5, 128.3, 126.1, 126.1, 126.0, 126.0, 125.2, 124.1, 124.0, 124.0, 123.9, 123.4, 123.3, 122.5, 111.0, 110.8, 110.0, 55.8, 46.2, 45.8, 42.6, 42.1, 42.1, 39.9, 28.8, 28.8, 25.7, 23.8; ^{19}F NMR (377 MHz, $CDCl_3$) δ -62.6, -116.9; MS (ESI) *m/z* 500.0 $[M+H]^+$; HRMS (ESI) found *m/z* 500.16332 $[M+H]^+$, calcd for $C_{23}H_{26}F_4N_3O_3S^+$ *m/z* 500.16310; $[\alpha]_D^{21}$ = -73.2° (dichloromethane).

Compound **2** (31 mg, 83% isolated yield, white solid): ^{1}H NMR (400 MHz, $CDCl_3$) δ 7.53 – 7.48 (m, 2H), 7.33 (bs, 1H), 7.28 – 7.24 (m, 3H), 7.20 (dd, *J* = 1.7, 8.7 Hz, 1H), 4.20 (t, *J* = 7.3 Hz, 1H), 4.02 (s, 2H), 3.24 – 3.06 (m, 5H), 2.99 (d, *J* = 7.3 Hz, 2H), 2.88 – 2.70 (m, 2H), 2.67 – 2.56 (m, 1H), 1.79 – 1.52 (m, 4H), 1.26 (bs, 1H); ^{13}C NMR (101 MHz, $CDCl_3$): δ 168.1, 160.0, 157.5, 139.8, 139.8, 139.8, 139.8, 139.0, 138.9, 138.8, 138.7, 129.9, 129.7, 129.4, 128.9, 128.7, 125.4, 125.3, 125.3, 125.3, 123.4, 123.4, 122.7, 111.0, 110.7, 55.7, 46.2, 45.8, 42.8, 42.4, 42.3, 39.9, 29.0, 29.0, 25.7, 23.9; ^{19}F NMR (377 MHz, $CDCl_3$): δ -62.53, -117.11; MS (ESI) *m/z* 500.1 $[M+H]^+$; HRMS (ESI) found *m/z* 500.16353 $[M+H]^+$, calcd for $C_{23}H_{26}F_4N_3O_3S^+$ *m/z* 500.16310; $[\alpha]_D^{21}$ = -91.3° (dichloromethane).

Compound **3** (35 mg, 91% isolated yield, off-white solid): ^{1}H NMR (400 MHz, $CDCl_3$) δ 7.58 (d, *J* = 7.7 Hz, 1H), 7.43 – 7.28 (m, 4H), 7.18 – 7.13 (m, 1H), 4.30 (t, *J* = 7.7 Hz, 1H), 4.02 (s, 2H), 3.23 (t, *J* = 6.3 Hz, 3H), 3.18 – 3.00 (m, 4H), 2.84 – 2.73 (m, 2H), 2.68 – 2.61 (m, 1H), 1.81 – 1.57 (m, 4H), 1.24 (bs, 1H); ^{13}C NMR (101 MHz, $CDCl_3$) δ 168.7, 160.0, 157.5, 139.0, 138.9, 138.7, 138.7, 134.1, 133.3, 133.2, 131.6, 129.0, 128.7, 128.6, 128.5, 127.3, 126.0, 125.9, 125.8, 123.4, 123.4, 123.1, 111.0, 110.8, 55.2, 46.0, 45.9, 42.8, 42.4, 42.4, 36.7, 30.9, 29.0, 25.8, 23.9; ^{19}F NMR (377 MHz, $CDCl_3$) δ -62.6, -117.1; MS (ESI) *m/z* 500.1 $[M+H]^+$; HRMS (ESI) found *m/z* 500.16319 $[M+H]^+$, calcd for $C_{23}H_{26}F_4N_3O_3S^+$ *m/z* 500.16310; $[\alpha]_D^{21}$ = -74.0° (dichloromethane).

Compound **4** (47 mg, 69% isolated yield, off-white solid): ^{1}H NMR (400 MHz, $CDCl_3$): δ 7.34 – 7.31 (m, 1H), 7.20 (dd, *J* = 1.8, 8.8 Hz, 1H), 7.11 (t, *J* = 7.9 Hz, 1H), 7.03 – 6.98 (m, 1H), 6.94 – 6.88 (m, 2H), 4.16 (dd, *J* = 6.7, 8.5 Hz, 1H), 4.03 (bs, 2H), 3.22 – 3.01 (m, 5H), 2.94 – 2.73 (m, 4H), 2.49 – 2.38 (m, 1H), 2.27 (s, 3H), 1.71 – 1.45 (m, 4H), 1.26 (bs, 1H); ^{13}C NMR (101 MHz, $CDCl_3$) δ 168.7, 160.0, 157.5, 139.1, 139.1, 138.7, 138.6, 138.0, 135.5, 130.1, 128.4, 128.3, 128.2, 127.8, 126.4, 123.4, 123.4, 111.1, 110.8, 56.2, 46.1, 45.7, 42.7, 42.2, 42.2, 40.4, 28.9, 25.7, 23.9, 21.3; ^{19}F NMR (377 MHz, $CDCl_3$) δ –117.2; MS (ESI) *m/z* 446.1 $[M+H]^+$; HRMS (ESI) found *m/z* 446.19004 $[M+H]^+$, calcd for $C_{23}H_{29}FN_3O_3S^+$ *m/z* 446.19006; $[\alpha]_D^{21}$ = -91.1° (dichloromethane).

This article is protected by copyright. All rights reserved.

Accepted Manuscript

Compound **5** (14 mg, 81% isolated yield, off-white solid): ^{1}H NMR (400 MHz, $CDCl_3$) δ 7.32 – 7.29 (bs, 1H), 7.22 – 7.14 (m, 3H), 7.08 – 7.00 (m, 2H), 4.19 – 4.13 (t, *J* = 7.4 Hz, 1H), 4.02 (s, 2H), 3.28 – 3.09 (m, 5H), 2.91 (d, *J* = 7.4 Hz, 2H), 2.85 – 2.76 (q, *J* = 6.1 Hz, 2H), 2.66 – 2.56 (m, 1H), 1.79 – 1.58 (m, 4H), 1.26 (bs, 1H); ^{13}C NMR (126 MHz, $CDCl_3$) δ 168.4, 159.8, 157.8, 138.8, 138.8, 138.8, 137.7, 134.2, 129.7, 129.4, 128.6, 128.5, 127.7, 127.3, 123.4, 123.4, 111.0, 110.8, 55.9, 46.2, 45.9, 42.8, 42.3, 42.3, 39.9, 28.9, 28.9, 25.8, 23.9; ^{19}F NMR (377 MHz, $CDCl_3$) δ -117.0; MS (ESI) *m/z* 466.1 $[M+H]^+$; HRMS (ESI) found *m/z* 466.13652 $[M+H]^+$, calcd for $C_{22}H_{26}ClFN_3O_3S^+$ *m/z* 466.13674; $[\alpha]_D^{21}$ = -88.9° (dichloromethane).

Compound **6** (18 mg, 72% isolated yield, off-white solid): ^{1}H NMR (400 MHz, $CDCl_3$) δ 7.35 – 7.29 (m, 2H), 7.24 – 7.16 (m, 2H), 7.14 – 7.06 (m, 2H), 4.16 (t, *J* = 7.5 Hz, 1H), 4.05 (s, 2H), 3.28 – 3.10 (m, 5H), 2.88 (d, *J* = 7.5 Hz, 2H), 2.85 – 2.78 (m, 2H), 2.66 – 2.55 (m, 1H), 1.79 – 1.58 (m, 4H) 1.26 (bs, 1H); ^{13}C NMR (126 MHz, $CDCl_3$) δ 168.4, 159.7, 157.8, 138.9, 138.9, 138.7, 138.6, 138.0, 132.3, 130.2, 130.0, 128.8, 128.3, 128.2, 128.2, 123.3, 123.3, 122.4, 111.0, 110.8, 55.9, 46.2, 45.9, 42.7, 42.2, 42.2, 39.8, 39.7, 29.7, 29.3, 28.7, 25.8, 23.9; ^{19}F NMR (377 MHz, $CDCl_3$) δ -117.1; MS (ESI) *m/z* 511.9 $[M+H]^+$; HRMS (ESI) found *m/z* 510.08574 $[M+H]^+$, calcd for $C_{22}H_{26}BrFN_3O_3S^+$ *m/z* 510.08523; $[\alpha]_D^{21}$ = -50.8° (dichloromethane).

Compound **7** (13 mg, 64% isolated yield, white solid): ^{1}H NMR (500 MHz, $CDCl_3$) δ 7.33 (bs, 1H), 7.25 – 7.18 (m, 4H), 7.14 – 7.09 (m, 2H), 4.16 (dd, *J* = 8.9, 6.2 Hz, 1H), 4.02 (bs, 2H), 3.17 – 2.87 (m, 7H), 2.85 – 2.73 (m, 2H), 2.44 – 2.39 (m, 1H), 1.67 – 1.56 (m, 3H), 1.52 – 1.45 (m, 1H) 1.25 (bs, 1H); ^{13}C NMR (126 MHz, $CDCl_3$) δ 168.8, 160.1, 158.1, 139.2, 139.2, 139.1, 135.9, 129.8, 129.1, 128.9, 128.8, 127.5, 123.8, 123.8, 111.4, 111.2, 56.5, 46.4, 46.0, 43.2, 42.8, 42.7, 40.9, 29.4, 29.3, 26.0, 24.2. ^{19}F NMR (377 MHz, $CDCl_3$) δ -117.3; MS (ESI) *m/z* 432.1 $[M+H]^+$; HRMS (ESI) found *m/z* 454.15748 $[M+Na]^+$, calcd for $C_{22}H_{26}FN_3O_3SNa^+$ *m/z* 545.15766; $[\alpha]_D^{21}$ = -67.1° (dichloromethane).

Compound **8** (25 mg, 85% isolated yield, off-white solid): ^{1}H NMR (500 MHz, $CDCl_3$) δ 7.81 – 7.76 (m, 1H), 7.73 – 7.68 (m, 2H), 7.54 (bs, 1H), 7.48 – 7.42 (m, 2H), 7.25 – 7.21 (m, 2H), 7.16 (dd, *J* = 8.7, 1.7 Hz, 1H), 4.30 (t, *J* = 7.5 Hz, 1H), 3.93 – 3.86 (m, 2H), 3.26 – 3.14 (m, 3H), 3.07 (dd, *J* = 7.5, 1.8 Hz, 2H), 3.01 (t, *J* = 5.9 Hz, 2H), 2.71 – 2.55 (m, 3H), 1.70 – 1.50 (m, 3H), 1.45 – 1.38 (m, 1H), 1.25 (bs, 1H); ^{13}C NMR (126 MHz, $CDCl_3$) δ 168.8, 159.6, 157.6, 138.9, 138.9, 138.7, 138.6, 133.3, 133.2, 132.3, 128.5, 128.4, 128.2, 128.0, 127.6, 127.5, 127.4, 126.2, 125.8, 123.2, 123.2, 110.9, 110.7, 56.2, 46.1, 45.8, 42.7, 42.2, 42.2, 40.4, 28.7, 28.7, 25.7, 23.9; ^{19}F NMR (377 MHz, $CDCl_3$) δ -117.4; MS (ESI) *m/z* 482.1 $[M+H]^+$; HRMS (ESI) found *m/z* 482.19176 $[M+H]^+$, calcd for $C_{26}H_{29}FN_3O_3S^+$ *m/z* 482.19136; $[\alpha]_D^{21}$ = -97.1° (dichloromethane).

Compound **9** (18 mg, 75% isolated yield, off-white solid): ^{1}H NMR (400 MHz, $CDCl_3$) δ 7.43 (bs, 1H), 7.34 (dd, *J* = 8.7, 1.7 Hz, 1H), 4.05 (s, 2H), 3.67 (s, 2H), 3.43 (t, *J* = 6.8 Hz, 2H), 3.29 (t, *J* = 6.8 Hz, 2H), 3.13 (t, *J* = 5.9 Hz, 2H), 2.85 (t, *J* = 5.9 Hz, 2H), 2.01 – 1.92 (m, 2H), 1.90 – 1.81 (m, 2H), 1.35 (t, *J* = 7.3 Hz, 1H); ^{13}C NMR (101 MHz, $CDCl_3$) δ 164.7, 160.3, 157.8, 139.1, 139.1, 137.8, 137.8, 129.0, 128.8, 123.5, 123.5, 111.3, 111.0, 46.2, 45.9, 45.4, 44.3, 42.8, 42.5, 42.4, k 29.0, 25.8, 24.1; ^{19}F NMR (377 MHz, $CDCl_3$) δ -117.0; MS (ESI) *m/z* 342.0 $[M+H]^+$; HRMS (ESI) found *m/z* 342.12923 $[M+H]^+$, calcd for $C_{15}H_{22}N_3O_3S^+$ *m/z* 342.12876.

Compound **10** (42 mg, 77% isolated yield, off-white solid): ^{1}H NMR (400 MHz, $CDCl_3$) δ 7.29 – 7.26 (m, 1H), 7.25 – 7.19 (m, 3H), 7.13 (dd, *J* = 8.6, 1.8 Hz, 1H), 7.09 – 7.02 (m, 2H), 5.45 (bs, 1H), 4.03 (s, 2H), 3.77 (t, *J* = 7.0 Hz, 1H), 3.12 (t, *J* = 5.9 Hz, 2H), 2.95 (qd, *J* = 13.8, 7.0 Hz, 2H), 2.83 – 2.76 (m, 2H), 2.04 – 1.97 (m, 3H), 1.80 – 1.71 (m, 6H), 1.67 – 1.55 (m, 6H), 1.26 (bs, 1H); ^{13}C NMR (101 MHz, $CDCl_3$) δ 168.5, 160.2, 157.7, 138.9, 138.8, 138.2, 138.1, 135.8, 129.3, 128.8, 128.7, 128.7, 128.5, 127.2, 123.5, 123.5, 111.1, 110.9, 58.6, 52.1, 42.7, 42.3, 42.3, 41.1, 39.4, 36.2, 29.3, 28.8, 28.8; ^{19}F NMR (377 MHz, $CDCl_3$) δ -116.6; MS (ESI) *m/z* 512.1 $[M+H]^+$; HRMS (ESI) found *m/z* 512.23804 $[M+H]^+$, calcd for $C_{28}H_{35}FN_3O_3S^+$ *m/z* 512.23831; $[\alpha]_D^{21}$ = -19.1° (dichloromethane).

Compound **11** (39 mg, 81% isolated yield, white solid): ^{1}H NMR (400 MHz, $CDCl_3$) δ 7.35 (bs, *J* = 1.6 Hz, 1H), 7.30 – 7.22 (m, 4H), 7.15 – 7.10 (m, 2H), 4.05 (s, 2H), 3.90 (dd, *J* = 9.0, 6.1 Hz, 1H), 3.82 – 3.64 (m, 3H), 3.13 (t, *J* = 5.9 Hz, 2H), 3.07 (td, *J* = 8.9, 6.2 Hz, 1H), 2.95 – 2.76 (m, 4H), 2.08 – 1.99 (m, 1H), 1.97 – 1.83 (m, 1H), 1.30 – 1.22 (m, 1H); ^{13}C NMR (101 MHz, $CDCl_3$) δ 169.2, 160.1, 157.6, 139.1, 139.0, 138.9, 138.8, 135.7, 129.4, 128.7, 128.5, 128.5, 127.2, 123.4, 123.3, 111.0, 110.8, 53.7, 49.7, 47.6, 42.8, 42.4, 42.3, 40.2, 29.0, 28.9, 15.2; ^{19}F NMR (377 MHz, $CDCl_3$) δ -117.2; MS (ESI) *m/z* 418.2 $[M+H]^+$; HRMS (ESI) found *m/z* 418.16006 $[M+H]^+$, calcd for $C_{21}H_{25}FN_3O_3S^+$ *m/z* 418.15965; $[\alpha]_D^{21}$ = -87.0° (dichloromethane).

Compound **12** (47 mg, 96% isolated yield, off-white solid): ^{1}H NMR (400 MHz, $CDCl_3$) δ 7.34 – 7.31 (m, 1H), 7.28 – 7.18 (m, 4H), 7.16 – 7.09 (m, 2H), 4.41 (dd, *J* = 7.8, 6.6 Hz, 1H), 4.02 (s, 2H), 3.36 – 3.26 (m, 1H), 3.26 – 3.17 (m, 1H), 3.10 (t, *J* = 5.9 Hz, 2H), 3.04 – 2.72 (m, 6H), 1.51 – 1.07 (m, 6H), 0.99 – 0.80 (m, 1H); ^{13}C NMR (101 MHz, $CDCl_3$) δ 168.3, 160.0, 157.6, 138.9, 138.8, 138.8, 138.7, 135.5, 129.6, 128.6, 128.5, 128.5, 127.2, 123.5, 123.5, 111.2, 111.0, 53.6, 46.3, 43.1, 42.8, 42.4, 42.3, 40.9, 29.0, 29.0, 25.6, 25.1, 24.0; ^{19}F NMR (377 MHz, $CDCl_3$) δ -117.2; MS (ESI) *m/z* 446.1 $[M+H]^+$; HRMS (ESI) found *m/z* 446.19111 $[M+H]^+$, calcd for $C_{23}H_{29}FN_3O_3S^+$ *m/z* 446.19136; $[\alpha]_D^{21}$ = -92.0° (dichloromethane).

Compound **13** (37 mg, 91% isolated yield, slightly yellow solid): ^{1}H NMR (400 MHz, $CDCl_3$) δ 7.34 (s, *J* = 7.8 Hz, 1H), 7.30 – 7.20 (m, 4H), 7.16 – 7.09 (m, 2H), 4.39 (dd, *J* = 9.4, 5.8 Hz, 1H), 4.03 (s, 2H), 3.47 – 3.28 (m, 3H), 3.28 – 3.07 (m, 4H), 3.04 – 2.64 (m, 7H), 1.25 (bs, 1H); ^{13}C NMR (126 MHz, $CDCl_3$) δ 169.0, 159.8, 157.9, 139.0, 139.0, 138.9, 138.8, 135.4, 129.6, 129.0, 128.8, 128.7, 127.5, 123.4, 123.4, 111.1, 110.9, 66.2, 65.6, 53.3, 45.7, 42.8, 42.4, 42.4, 42.2, 41.0, 29.1, 29.0; ^{19}F NMR (377 MHz, $CDCl_3$) δ -117.3; MS (ESI) *m/z* 448.1 $[M+H]^+$; HRMS (ESI) found *m/z* 448.17145 $[M+H]^+$, calcd for $C_{22}H_{27}FN_3O_4S^+$ *m/z* 448.17063; $[\alpha]_D^{21}$ = -86.2° (dichloromethane).

Compound **14** (41 mg, 85% isolated yield, white solid): ^{1}H NMR (400 MHz, $CDCl_3$) δ 7.34 – 7.30 (m, 1H), 7.26 – 7.19 (m, 4H), 7.15 – 7.09 (m, 2H), 4.34 (dd, *J* = 7.7, 6.5 Hz, 1H), 4.01 (s, 2H), 3.31 – 3.20 (m, 1H), 3.13 – 3.00 (m, 3H), 2.99 – 2.82 (m, 4H), 2.78 (q, *J* = 5.2 Hz, 2H), 1.25 (bs, 1H), 0.92 (t, *J* = 7.1 Hz, 3H), 0.84 (t, *J* = 7.1 Hz, 3H); ^{13}C NMR (126 MHz, $CDCl_3$) δ 169.5, 159.8, 157.9, 139.3, 139.2, 138.8, 138.7, 135.6, 129.5, 128.6, 128.5, 128.5, 127.2, 123.3, 123.3, 111.1, 110.9, 54.1, 42.8, 42.3, 42.3, 41.5, 40.9, 40.6, 29.0, 28.9, 13.7, 12.6; ^{19}F NMR (377 MHz, $CDCl_3$) δ -117.3; MS (ESI) *m/z* 434.1 $[M+H]^+$; HRMS (ESI) found *m/z* 434.19037 $[M+H]^+$, calcd for $C_{22}H_{29}FN_3O_3S^+$ *m/z* 434.19082; $[\alpha]_D^{21}$ = -64.5° (dichloromethane).

Compound **15** (38 mg, 95% isolated yield, off-white solid): ^{1}H NMR (400 MHz, $CDCl_3$) δ 7.31 (bs, 1H), 7.26 – 7.18 (m, 4H), 7.13 – 7.08 (m, 2H), 4.42 (dd, *J* = 7.9, 6.8 Hz, 1H), 4.03 (s, 2H), 3.11 (t, *J* = 5.9 Hz, 2H), 2.91 (d, *J* = 8.4 Hz, 2H), 2.80 (q, *J* = 5.7 Hz, 2H), 2.67 (s, 3H), 2.48 (s, 3H), 1.24 (bs, 1H); ^{13}C NMR (101 MHz, $CDCl_3$) δ 170.3, 160.0, 157.6, 139.0, 139.0, 138.8, 138.7, 135.6, 129.3, 128.6, 128.5, 128.4, 127.2, 123.3, 123.3, 111.0, 110.7, 54.0, 42.8, 42.3, 42.3, 40.5, 36.5, 35.5, 28.9, 28.9; ^{19}F NMR (377 MHz, $CDCl_3$) δ -117.3; MS (ESI) *m/z* 406.1 $[M+H]^+$; HRMS (ESI) found *m/z* 406.16060 $[M+H]^+$, calcd for $C_{20}H_{25}FN_3O_3S^+$ *m/z* 406.16006; $[\alpha]_D^{21}$ = -91.1° (dichloromethane).

Compound **16** (31 mg, 81% isolated yield, off-white solid): ^{1}H NMR (400 MHz, $CDCl_3$) δ 7.34 (bs, 1H), 7.30 – 7.19 (m, 4H), 7.12 – 7.07 (m, 2H), 4.04 (s, 1H), 3.23 (t, *J* = 6.9 Hz, 1H), 3.11 (t, *J* = 5.9 Hz, 1H), 2.86 – 2.75 (m, 4H), 2.06 (bs, 1H), 1.25 (bs, 1H); ^{13}C NMR (101 MHz, $CDCl_3$) δ 160.3, 157.8, 138.9, 138.9, 138.7, 138.6, 137.6, 128.8, 128.8, 128.7, 128.7, 128.5, 126.9, 123.3, 123.3, 111.1, 110.8, 44.2, 42.7, 42.3, 42.3, 35.8, 28.9, 28.9; ^{19}F NMR (377 MHz, $CDCl_3$) δ -116.9. MS (ESI) *m/z* 335.1 $[M+H]^+$; HRMS

This article is protected by copyright. All rights reserved.

Accepted Manuscript

(ESI) found *m/z* 335.12305 $[M+H]^+$, calcd for $C_{17}H_{20}FN_2O_2S^+$ *m/z* 335.12295.

Compound **17** (88 mg, 88%, white solid): ^{1}H NMR (500 MHz, $CDCl_3$) δ 7.84 – 7.80 (m, 2H), 7.56 – 7.51 (m, 1H), 7.49 – 7.43 (m, 2H), 7.27 – 7.19 (m, 3H), 7.17 – 7.12 (m, 2H), 5.95 – 5.90 (d, *J* = 9.5 Hz, 1H), 4.17 – 4.05 (td, *J* = 9.5, 5.9 Hz, 1H), 3.14 – 3.06 (m, 1H), 3.03 – 2.89 (m, 3H), 2.87 – 2.80 (m, 1H), 2.32 – 2.24 (m, 1H), 1.57 – 1.36 (m, 4H); ^{13}C NMR (126 MHz, $CDCl_3$) δ 168.4, 139.9, 135.7, 132.6, 129.4, 128.8, 128.4, 127.2, 127.2, 56.0, 45.9, 45.5, 40.7, 25.6, 23.7; MS (ESI) *m/z* 359.0 $[M+H]^+$; HRMS (ESI) found *m/z* 381.12487 $[M+Na]^+$, calcd for $C_{19}H_{22}N_2O_3SNa^+$ *m/z* 381.12433; $[\alpha]_D^{21}$ = -125.8° (dichloromethane).

Compound **18** (94 mg, 94% isolated yield, white solid): ^{1}H NMR (500 MHz, $CDCl_3$) δ 7.62 (dt, *J* = 8.0, 1.7, 1.0 Hz, 1H), 7.51 (dt, *J* = 8.0, 2.5, 1.7 Hz, 1H), 7.45 (td, *J* = 8.0, 5.2 Hz, 1H), 7.28 – 7.20 (m, 4H), 7.17 – 7.13 (m, 2H), 6.27 (d, *J* = 9.7 Hz, 1H), 4.20 (ddd, *J* = 9.7, 8.4, 6.7 Hz, 1H), 3.23 – 3.11 (m, 1H), 3.07 – 2.94 (m, 4H), 2.45 – 2.36 (m, 1H), 1.68 – 1.42 (m, 4H); ^{13}C NMR (126 MHz, $CDCl_3$) δ 168.3, 163.1, 161.1, 142.4, 142.3, 135.6, 130.7, 130.7, 129.4, 128.5, 127.2, 123.0, 122.9, 119.7, 119.6, 114.5, 114.3, 56.2, 46.0, 45.7, 40.5, 25.7, 23.8; ^{19}F NMR (377 MHz, $CDCl_3$) δ -109.8; MS (ESI) *m/z* 376.9 $[M+H]^+$; HRMS (ESI) found *m/z* 399.11732 $[M+Na]^+$, calcd for $C_{19}H_{21}FN_2O_3SNa^+$ *m/z* 399.11546; Optical rotation $[\alpha]_D^{21}$ = -116.4° (dichloromethane).

Compound **19** (78 mg, 78% isolated yield, white solid): ^{1}H NMR (500 MHz, $CDCl_3$) δ 7.83 – 7.77 (m, 2H), 7.27 – 7.18 (m, 3H), 7.15 – 7.06 (m, 4H), 6.15 (d, *J* = 9.8 Hz, 1H), 4.19 – 4.09 (m, 1H), 3.18 – 3.08 (m, 1H), 3.05 – 2.89 (m, 4H), 2.44 – 2.35 (m, 1H), 1.63 – 1.51 (m, 3H), 1.50 – 1.41 (m, 1H); ^{13}C NMR (126 MHz, $CDCl_3$) δ 168.6, 166.0, 163.9, 136.2, 136.2, 135.6, 130.0, 129.9, 129.4, 128.5, 127.2, 116.0, 115.8, 56.0, 46.0, 45.7, 40.4, 25.6, 23.8; ^{19}F NMR (377 MHz, $CDCl_3$) δ -105.4; MS (ESI) *m/z* 377.1 $[M+H]^+$; HRMS (ESI) found *m/z* 399.11607 $[M+Na]^+$, calcd for $C_{19}H_{21}FN_2O_3SNa^+$ *m/z* 399.11546; $[\alpha]_D^{21}$ = -96.7° (dichloromethane).

Compound **20** (88 mg, 99% isolated yield, white solid): ^{1}H NMR (500 MHz, $CDCl_3$) δ 7.32 (d, *J* = 2.3 Hz, 1H), 7.30 – 7.19 (m, 4H), 7.17 – 7.11 (m, 2H), 6.89 (d, *J* = 8.5 Hz, 1H), 5.81 (d, *J* = 9.8 Hz, 1H), 4.33 – 4.21 (m, 4H), 4.13 (td, *J* = 5.9, 9.55 Hz, 1H), 3.18 – 3.03 (m, 2H), 3.01 – 2.89 (m, 3H), 2.38 – 2.29 (m, 1H), 1.67 – 1.53 (m, 3H), 1.50 – 1.39 (m, 1H); ^{13}C NMR (126 MHz, $CDCl_3$) δ 168.6, 147.2, 143.2, 135.8, 132.5, 129.4, 128.4, 127.1, 120.9, 117.5, 116.8, 64.5, 64.1, 56.0, 45.9, 45.6, 40.6, 25.7, 23.8; MS (ESI) *m/z* 417.0 $[M+H]^+$; HRMS (ESI) found *m/z* 439.13019 $[M+Na]^+$, calcd for $C_{21}H_{24}N_2O_5SNa^+$ *m/z* 439.13036. $[\alpha]_D^{21}$ = -106.4° (dichloromethane).

Compound **21** (87 mg, 98% isolated yield, white solid): ^{1}H NMR (500 MHz, $CDCl_3$) δ 9.20 (s, 1H), 8.44 (dd, *J* = 0.6, 1.90 Hz, 1H), 8.18 (dd, *J* = 0.6, 8.6 Hz, 1H), 7.92 (dd, *J* = 1.9, 8.6 Hz, 1H), 7.23 – 7.14 (m, 3H), 7.14 – 7.09 (m, 2H), 6.21 (bs, 1H), 4.19 (dd, *J* = 6.4, 8.7 Hz, 1H), 3.10 – 2.93 (m, 3H), 2.93 – 2.77 (m, 2H), 2.42 – 2.33 (m, 1H), 1.51 – 1.36 (m, 3H), 1.35 – 1.24 (m, 1H); ^{13}C NMR (126 MHz, $CDCl_3$) δ 168.4, 157.9, 155.4, 137.4, 135.6, 133.8, 129.4, 128.4, 127.2, 125.0, 123.9, 122.0, 56.2, 45.9, 45.6, 40.5, 25.6, 23.7; MS (ESI) *m/z* 416.1 $[M+H]^+$; HRMS (ESI) found *m/z* 438.09165 $[M+Na]^+$, calcd for $C_{20}H_{21}N_3O_3S_2Na^+$ *m/z* 438.09220. $[\alpha]_D^{21}$ = -107.9° (dichloromethane).

Compound **22** (89 mg, 97% isolated yield, white solid): ^{1}H NMR (500 MHz, $CDCl_3$) δ 7.62 – 7.55 (m, 2H), 7.25 – 7.17 (m, 3H), 7.15 – 7.10 (m, 2H), 6.74 (d, *J* = 8.3 Hz, 1H), 5.91 (d, *J* = 9.9 Hz, 1H), 4.63 (t, *J* = 8.8 Hz, 2H), 4.16 – 4.06 (m, 1H), 3.29 – 3.09 (m, 3H), 3.05 – 2.88 (m, 4H), 2.38 – 2.30 (m, 1H), 1.60 – 1.50 (m, 3H), 1.47 – 1.40 (m, 1H); ^{13}C NMR (126 MHz, $CDCl_3$) δ 168.8, 163.7, 135.8, 131.5, 129.4, 128.7, 128.4, 128.2, 127.1, 124.6, 108.8, 72.3, 55.9, 45.9, 45.6, 40.5, 29.0, 25.6, 23.8; MS (ESI) *m/z* 401.0 $[M+H]^+$; HRMS (ESI) found *m/z* 423.13553 $[M+Na]^+$, calcd for $C_{21}H_{24}N_2O_4SNa^+$ *m/z* 423.13553. $[\alpha]_D^{21}$ = -124.2° (dichloromethane).

Compound **23** (56 mg, 99% isolated yield, off-white solid): ^{1}H NMR (400 MHz, $CDCl_3$) δ 7.56 – 7.48 (m, 2H), 7.26 – 7.16 (m, 3H), 7.15 – 7.04 (m, 3H), 4.13 (dd, *J* = 8.9, 6.2 Hz, 1H), 4.07 (s, 2H), 3.21 – 3.06 (m, 3H), 3.06 – 2.71 (m, 7H), 2.40 – 2.26 (m, 1H), 1.64 – 1.48 (m, 3H), 1.50 – 1.36 (m, 1H), 1.23 (bs, 1H); ^{13}C NMR (101 MHz, $CDCl_3$) δ 168.7, 140.1, 137.8, 135.8, 135.6, 129.4, 128.4, 128.0, 127.1, 126.8, 124.5, 56.0, 47.8, 45.9, 45.6, 43.2, 40.5, 28.8, 25.7, 23.8; MS (ESI) *m/z* 414.1 $[M+H]^+$; HRMS (ESI) found *m/z* 414.18487 $[M+H]^+$, calcd for $C_{22}H_{28}N_3O_3S^+$ *m/z* 414.18514. $[\alpha]_D^{21}$ = -96.9° (dichloromethane).

Compound **24** (153 mg, 86% isolated yield, colorless oil): ^{1}H NMR (400 MHz, $CDCl_3$) δ 7.51 – 7.45 (m, 2H), 7.25 – 7.17 (m, 3H), 7.15 – 7.08 (m, 3H), 5.77 (d, *J* = 9.6 Hz, 1H), 4.08 (td, *J* = 9.6, 5.9 Hz, 1H), 3.14 – 3.03 (m, 1H), 3.02 – 2.85 (m, 3H), 2.85 – 2.66 (m, 5H), 2.31 – 2.19 (m, 1H), 1.78 (p, *J* = 3.3 Hz, 4H), 1.58 – 1.32 (m, 4H); ^{13}C NMR (126 MHz, $CDCl_3$) δ 168.6, 142.6, 137.9, 136.7, 135.8, 129.4, 129.4, 128.4, 127.8, 127.1, 124.2, 55.9, 45.8, 45.4, 40.7, 29.5, 29.3, 25.6, 23.8, 22.7, 22.7; MS (ESI) *m/z* 413.1 $[M+H]^+$; HRMS (ESI) found *m/z* 435.17130 $[M+Na]^+$, calcd for $C_{23}H_{28}O_3N_2SNa^+$ *m/z* 435.17183. $[\alpha]_D^{21}$ = -92.7° (dichloromethane).

Compound **25** (32 mg, 79% isolated yield, slightly yellow oil): ^{1}H NMR (400 MHz, $CDCl_3$); δ 7.30 – 7.23 (m, 2H), 7.19 – 7.09 (m, 3H), 7.09 – 7.02 (m, 2H), 6.27 (d, *J* = 8.5 Hz, 1H), 5.49 (d, *J* = 9.8 Hz, 1H), 3.94 (td, *J* = 9.8, 5.7 Hz, 1H), 3.25 (dd, *J* = 6.1, 5.0 Hz, 2H), 3.06 – 2.87 (m, 3H), 2.87 – 2.51 (m, 4H), 2.20 – 2.06 (m, 1H), 1.85 – 1.75 (m, 2H), 1.51 – 1.38 (m, 3H), 1.35 – 1.23 (m, 1H); ^{13}C NMR (101 MHz, $CDCl_3$) δ 168.1, 147.4, 135.0, 128.4, 127.9, 127.3, 126.0, 125.9, 124.1, 119.0, 111.2, 54.8, 44.8, 44.5, 40.5, 39.7, 25.9, 24.6, 22.8, 20.1; MS (ESI) *m/z* 414.0 $[M+H]^+$; HRMS (ESI) found *m/z* 436.16680 $[M+Na]^+$, calcd for $C_{22}H_{27}N_3O_3SNa^+$ *m/z* 436.16708; $[\alpha]_D^{21}$ = -134.3° (dichloromethane).

Compound **26** (62 mg, 95% isolated yield, off-white solid): ^{1}H NMR (500 MHz, $CDCl_3$) δ 7.53 (dd, *J* = 8.0, 2.0 Hz, 1H), 7.46 (bs, 1H), 7.26 – 7.18 (m, 3H), 7.17 – 7.09 (m, 3H), 4.12 (dd, *J* = 9.2, 6.0 Hz, 1H), 4.02 (q, *J* = 16.2 Hz, 2H), 3.20 – 3.08 (m, 3H), 3.06 – 2.88 (m, 4H), 2.83 (t, *J* = 6.0, 2H), 2.38 – 2.29 (m, 1H), 1.64 – 1.35 (m, 4H); ^{13}C NMR (126 MHz, $CDCl_3$) δ 168.6, 140.2, 137.3, 136.5, 135.7, 129.7, 129.4, 128.4, 127.1, 125.2, 124.7, 56.0, 47.9, 45.9, 45.5, 43.2, 40.6, 29.2, 25.6, 23.8; MS (ESI) *m/z* 414.1 $[M+H]^+$; HRMS (ESI) found *m/z* 414.18545 $[M+H]^+$, calcd for $C_{22}H_{28}N_3O_3S^+$ *m/z* 414.18514; $[\alpha]_D^{21}$ = -107.9° (dichloromethane).

Compound **27** (35 mg, 87% isolated yield, slightly yellow solid): ^{1}H NMR (400 MHz, $CDCl_3$) δ 7.56 (dd, *J* = 8.0, 1.8 Hz, 1H), 7.51 – 7.46 (m, 1H), 7.42 (dd, *J* = 9.4, 1.8 Hz, 1H), 7.26 – 7.17 (m, 3H), 7.16 – 7.08 (m, 2H), 4.19 (dd, *J* = 8.5, 6.6 Hz, 1H), 3.94 (s, 2H), 3.14 (dd, *J* = 13.0, 6.1 Hz, 1H), 3.10 – 2.99 (m, 2H), 3.00 – 2.84 (m, 2H), 2.50 – 2.36 (m, 1H), 1.71 – 1.54 (m, 3H), 1.54 – 1.41 (m, 1H); ^{13}C NMR (126 MHz, $CDCl_3$) δ 168.4, 161.0, 159.0, 140.5, 140.5, 135.6, 135.2, 135.1, 129.5, 129.5, 129.4, 128.5, 127.2, 123.1, 123.0, 114.3, 114.1, 56.2, 46.1, 45.7, 40.5, 40.0, 39.9, 25.7, 23.8; ^{19}F NMR (377 MHz, $CDCl_3$) δ -116.5; MS (ESI) *m/z* 406.1 $[M+H]^+$; HRMS (ESI) found *m/z* 406.16057 $[M+H]^+$, calcd for $C_{20}H_{25}FN_3O_3S^+$ *m/z* 406.16006; $[\alpha]_D^{21}$ = -82.2° (dichloromethane).

Compound **28** (69 mg, 75% isolated yield, white solid): ^{1}H NMR (500 MHz, DMSO-d_6) δ 8.39 (s, 1H), 8.14 (s, 1H), 7.95 (d, *J* = 8.5 Hz, 1H), 7.71 (d, *J* = 8.5 Hz, 2H), 7.58 (s, 1H), 7.28 – 7.09 (m, 4H), 4.10 (t, *J* = 7.6 Hz, 1H), 3.24 – 3.15 (m, 1H), 2.92 (dt, *J* = 6.9, 11.5 Hz, 1H), 2.88 – 2.66 (m, 4H), 1.71 – 1.60 (m, 1H), 1.52 - 1.45 (m, 3H); ^{13}C NMR (126 MHz, DMSO-d6) δ 168.0, 167.1, 143.5, 137.8, 137.0, 129.7, 128.6, 128.3, 127.1, 126.7, 56.1, 46.0, 45.6, 38.6, 25.2, 23.8; MS (ESI) *m/z* 402.0 $[M+H]^+$; HRMS (ESI) found *m/z* 424.13147 $[M+Na]^+$, calcd for $C_{20}H_{23}N_3O_4SNa^+$ *m/z* 424.13070; $[\alpha]_D^{21}$ = -91.7° (dichloromethane).

Compound **29** (20 mg, 99% isolated yield, TFA salt, white solid): ^{1}H NMR (500 MHz, CD_3OD) δ 7.67 (d, *J* = 1.5 Hz, 1H), 7.57 (dd, *J* = 9.2, 1.6 Hz, 1H), 4.47 (s, 2H), 3.57 (t, *J* = 6.3 Hz, 2H), 3.23 (t, *J* = 6.3 Hz, 2H); ^{13}C NMR (126 MHz, CD_3OD) δ 160.0, 158.0, 145.1, 145.0, 135.4, 135.3, 122.0, 122.0, 120.3, 120.1, 110.9, 110.7, 40.7, 39.3, 39.2, 24.5, 24.5; 19F NMR

This article is protected by copyright. All rights reserved.

Accepted Manuscript

(377 MHz, MeOD) δ -77.0 (CF_3COO^-), -118.1; MS (ESI) *m/z* 231.1 $[M+H]^+$; HRMS (ESI) found *m/z* 231.06035 $[M+H]^+$, calcd for $C_9H_{12}FN_2O_2S^+$ *m/z* 231.05922.

Compound **30** (943 mg, 80% isolated yield, yellow solid): ^1H NMR (400 MHz, $CDCl_3$) δ 7.32 – 7.26 (m, 2H), 7.25 – 7.18 (m, 3H), 3.71 (t, *J* = 7.2 Hz, 1H), 3.52 – 3.43 (m, 1H), 3.42 – 3.29 (m, 2H), 2.95 (dd, *J* = 13.1, 7.2 Hz, 1H), 2.84 – 2.75 (m, 2H), 1.86 – 1.60 (m, 6H). ^{13}C NMR (126 MHz, $CDCl_3$) δ 173.1, 137.9, 129.3, 128.4, 126.7, 55.2, 46.0, 45.8, 43.0, 25.9, 24.0. MS (ESI) *m/z* 219.0 $[M+H]^+$; HRMS (ESI) found *m/z* 241.13149 $[M+Na]^+$, calcd for $C_{13}H_{18}N_2ONa^+$ *m/z* 241.13168.

Acknowledgements

We thank the Netherlands Organization for Scientific Research (NWO, NCI-TA grant 731.015.202) for funding.

Keywords: Histone lysine methyltransferase • (*R*)-PFI-2 • SETD7 • Epigenetics • Structure-Activity Relationship

Conflict of interest

The authors declare no conflict of interest.

References

[1] A. J. Bannister, T. Kouzarides, *Cell Res.* **2011**, *21*, 381-395.
[2] K. A. Gelato, W. Fischle, *Biol. Chem.* **2008**, *389*, 353-363.
[3] E. L. Greer, Y. Shi, *Nat. Rev. Genet.* **2012**, *13*, 343-357.
[4] C. Martin, Y. Zhang, *Nat. Rev. Mol. Cell Biol.* **2005**, *6*, 838-849.
[5] K. Hyun, J. Jeon, K. Park, J. Kim, *Exp. Mol. Med.* **2017**, *49*, e324.
[6] M. Wong, P. Polly, T. Liu, *Am. J. Cancer. Res.* **2015**, *5*, 2823-2837.
[7] K. Nishioka, S. Chuikov, K. Sarma, H. Erdjument-Bromage, C. D. Allis, P. Tempst, D. Reinberg, *Genes Dev.* **2002**, *16*, 479-489.
[8] K. Subramanian, D. Jia, P. Kapoor-Vazirani, D. R. Powell, R. E. Collins, D. Sharma, J. Peng, X. Cheng, P. M. Vertino, *Mol. Cell* **2008**, *30*, 336-347.
[9] P. O. Esteve, H. G. Chin, J. Benner, G. R. Feehery, M. Samaranayake, G. A. Horwitz, S. E. Jacobsen, S. Pradhan, *Proc. Natl. Acad. Sci. USA* **2009**, *106*, 5076-5081.
[10] A. Kouskouti, E. Scheer, A. Staub, L. Tora, I. Talianidis, *Mol. Cell* **2004**, *14*, 175-182.
[11] D. R. Calnan, A. E. Webb, J. L. White, T. R. Stowe, T. Goswami, X. Shi, A. Espejo, M. T. Bedford, O. Gozani, S. P. Gygi, A. Brunet, *Aging* **2012**, *4*, 462-479.
[12] W. J. Zhang, X. N. Wu, T. T. Shi, H. T. Xu, J. Yi, H. F. Shen, M. F. Huang, X. Y. Shu, F. F. Wang, B. L. Peng, R. Q. Xiao, W. W. Gao, J. C. Ding, W. Liu, *Sci. Rep.* **2016**, *6*, 21718.
[13] L. Gaughan, J. Stockley, N. Wang, S. R. McCracken, A. Treumann, K. Armstrong, F. Shaheen, K. Watt, I. J. McEwan, C. Wang, R. G. Pestell, C. N. Robson, *Nucleic Acids Res.* **2011**, *39*, 1266-1279.
[14] I. Kassner, A. Andersson, M. Fey, M. Tomas, E. Ferrando-May, M. O. Hottiger, *Open Biol.* **2013**, *3*, 120173.
[15] C. Shen, D. Wang, X. Liu, B. Gu, Y. Du, F. Z. Wei, L. L. Cao, B. Song, X. Lu, Q. Yang, Q. Zhu, T. Hou, M. Li, L. Wang, H. Wang, Y. Zhao, Y. Yang, W. G. Zhu, *FASEB J.* **2015**, *29*, 4313-4323.
[16] J. K. Kurash, H. Lei, Q. Shen, W. L. Marston, B. W. Granda, H. Fan, D. Wall, E. Li, F. Gaudet, *Mol. Cell* **2008**, *29*, 392-400.
[17] a) J. Zhou, M. Xie, Y. Shi, B. H. Luo, G. H. Gong, J. N. Li, J. P. Wang, W. J. Zhao, Y. Zi, X. Y. Wu, J. F. Wen, *Oncol. Rep.* **2015**, *34*, 111-120; b) Y. Zhang, J. Liu, J. Lin, L. Zhou, Y. Song, B. Wei, X. Luo, Z. Chen, Y. Chen, J. Xiong, X. Xu, L. Ding, Q. Ye, *Oncotarget* **2016**, *7*, 9859-9875.
[18] F. Paneni, S. Costantino, R. Battista, L. Castello, G. Capretti, S. Chiandotto, G. Scavone, A. Villano, D. Pitocco, G. Lanza, M. Volpe, T. F. Luscher, F. Cosentino, *Circ. Cardiovasc. Genet.* **2015**, *8*, 150-158.
[19] a) F. Paneni, S. Costantino, R. Battista, L. Castello, G. Capretti, S. Chiandotto, G. Scavone, A. Villano, D. Pitocco, G. Lanza, M. Volpe, T. F. Lüscher, F. Cosentino, *Circ. Cardiovasc. Genet.* **2015**, *8*, 150; b) H. U. Kaniskan, M. L. Martini, J. Jin, *Chem. Rev.* **2017**; c) H. Ü. Kaniskan, K. D. Konze, J. Jin, *J. Med. Chem.* **2015**, *58*, 1596-1629; d) H. Ü. Kaniskan, J. Jin, *Curr. Opin. Chem. Biol.* **2017**, *39*, 100-108.
[20] Y. Takemoto, A. Ito, H. Niwa, M. Okamura, T. Fujiwara, T. Hirano, N. Handa, T. Umehara, T. Sonoda, K. Ogawa, M. Tariq, N. Nishino, S. Dan, H. Kagechika, T. Yamori, S. Yokoyama, M. Yoshida, *J. Med. Chem.* **2016**, *59*, 3650-3660.
[21] T. Fujiwara, K. Ohira, K. Urushibara, A. Ito, M. Yoshida, M. Kanai, A. Tanatani, H. Kagechika, T. Hirano, *Bioorg. Med. Chem.* **2016**, *24*, 4318-4323.
[22] H. Niwa, N. Handa, Y. Tomabechi, K. Honda, M. Toyama, N. Ohsawa, M. Shirouzu, H. Kagechika, T. Hirano, T. Umehara, S. Yokoyama, *Acta Crystallogr. D Biol. Crystallogr.* **2013**, *69*, 595-602.
[23] F. Meng, S. Cheng, H. Ding, S. Liu, Y. Liu, K. Zhu, S. Chen, J. Lu, Y. Xie, L. Li, R. Liu, Z. Shi, Y. Zhou, Y. C. Liu, M. Zheng, H. Jiang, W. Lu, H. Liu, C. Luo, *J. Med. Chem.* **2015**, *58*, 8166-8181.
[24] D. Barsyte-Lovejoy, F. Li, M. J. Oudhoff, J. H. Tatlock, A. Dong, H. Zeng, H. Wu, S. A. Freeman, M. Schapira, G. A. Senisterra, E. Kuznetsova, R. Marcellus, A. Allali-Hassani, S. Kennedy, J. P. Lambert, A. L. Couzens, A. Aman, A. C. Gingras, R. Al-Awar, P. V. Fish, B. S. Gerstenberger, L. Roberts, C. L. Benn, R. L. Grimley, M. J. Braam, F. M. Rossi, M. Sudol, P. J. Brown, M. E. Bunnage, D. R. Owen, C. Zaph, M. Vedadi, C. H. Arrowsmith, *Proc. Natl. Acad. Sci. USA* **2014**, *111*, 12853-12858.
[25] a) D. C. Lenstra, A. H. K. Al Temimi, J. Mecinović, *Bioorg. Med. Chem. Lett.* **2018**, *28*, 1234-1238; b) K. Guitot, T. Drujon, F. Burlina, S. Sagan, S. Beaupierre, O. Pamlard, R. H. Dodd, C. Guillou, G. Bolbach, E. Sachon, D. Guianvarc'h, *Anal. Bioanal. Chem.* **2017**, *409*, 3767-3777.
[26] *Chemical Computing Group Molecular Operating Environment (MOE),* https://www.chemcomp.com/.
[27] *Qiagen Molegro Virtual Docker v6.0,* https://www.qiagenbioinformatics.com/.
[28] *Schrödinger PyMOL,* https://pymol.org/.

Accepted Manuscript

This article is protected by copyright. All rights reserved.

10.1002/cmdc.201800242

WILEY-VCH

FULL PAPER

Entry for the Table of Contents

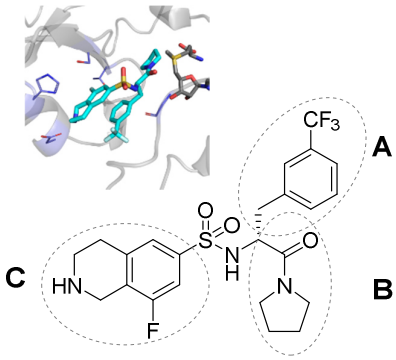

This work describes structure-activity relationship studies on (*R*)-PFI-2, the most potent inhibitor of biomedically important histone lysine methyltransferase SETD7. Synthesis and evaluation of 29 structural analogs of (*R*)-PFI-2 revealed key interactions that essentially contribute to excellent potency.

WILEY-VCH

Accepted Manuscript

This article is protected by copyright. All rights reserved.